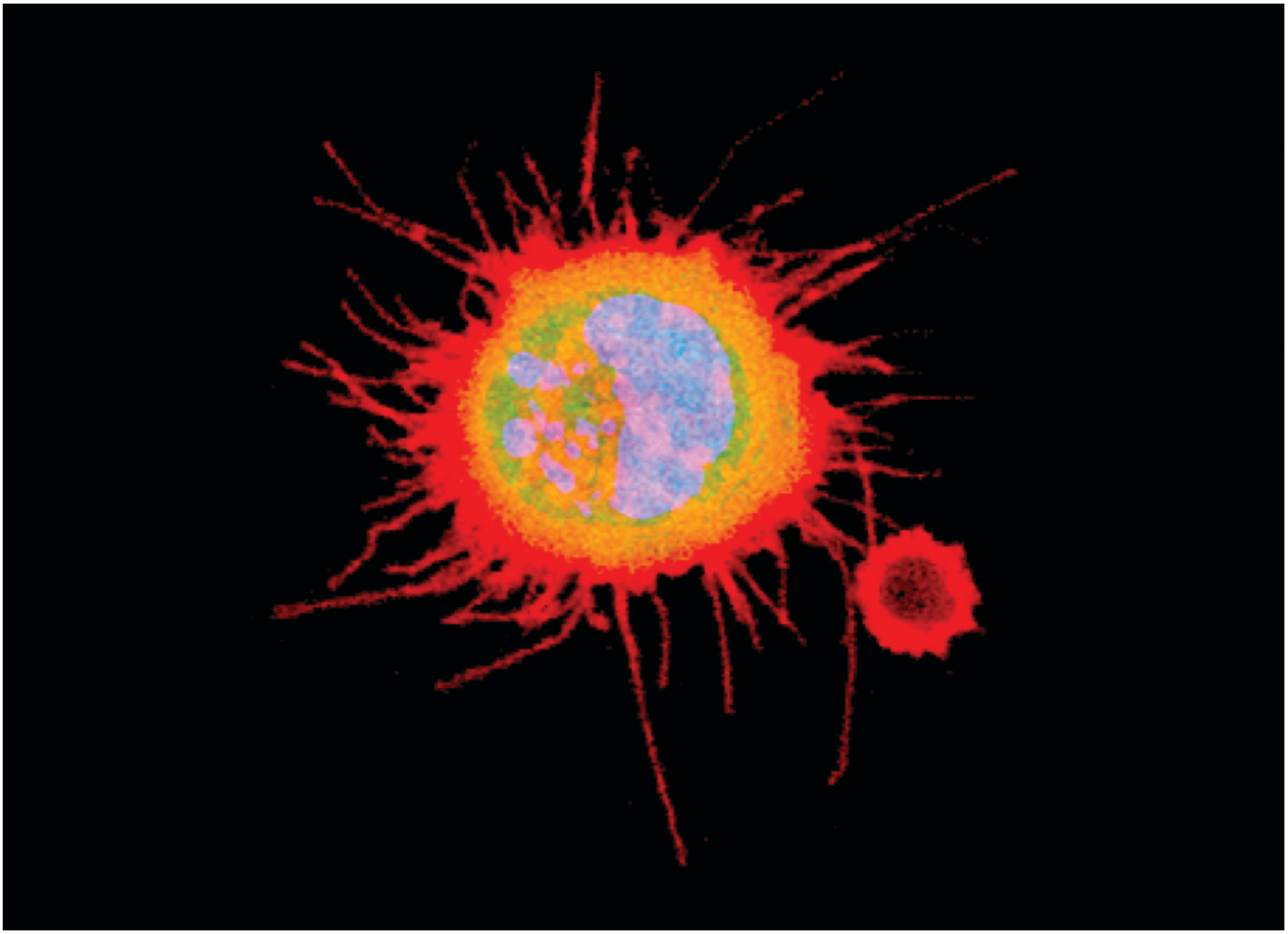

Featuring work from Dr. Stuart S. Martin's laboratory in the Marlene and Stewart Greenebaum NCI Comprehensive Cancer Center at the University of Maryland School of Medicine, Baltimore, Maryland, USA.

Partial thermal imidization of polyelectrolyte multilayer cell tethering surfaces (TetherChip) enables efficient cell capture and microtentacle fixation for circulating tumor cell analysis

Breast cancer cell isolated from blood and tethered onto TetherChip for rapid analysis of non-adherent, single-cell metastatic phenotypes. TetherChip is an engineered nanosurface comprised of a polyelectrolyte multilayer to prevent cell adhesion and a terminal lipid layer to simultaneously tether the cell membrane for spatial immobilization.

As featured in:

See Stuart S. Martin *et al.*, *Lab Chip*, 2020, **20**, 2872.

ROYAL SOCIETY OF CHEMISTRY

rsc.li/loc

Registered charity number: 207890

Lab on a Chip

PAPER

View Article Online
View Journal | View Issue

Cite this: *Lab Chip*, 2020, **20**, 2872

Partial thermal imidization of polyelectrolyte multilayer cell tethering surfaces (TetherChip) enables efficient cell capture and microtentacle fixation for circulating tumor cell analysis†

Julia A. Ju, ‡[a] Cornell J. Lee,‡[a] Keyata N. Thompson,[a] Eleanor C. Ory,[a] Rachel M. Lee, [a] Trevor J. Mathias, [ab] Stephen J. P. Pratt,[ac] Michele I. Vitolo, [abd] Christopher M. Jewell [ef] and Stuart S. Martin*[abdf]

The technical challenges of imaging non-adherent tumor cells pose a critical barrier to understanding tumor cell responses to the non-adherent microenvironments of metastasis, like the bloodstream or lymphatics. In this study, we optimized a microfluidic device (TetherChip) engineered to prevent cell adhesion with an optically-clear, thermal-crosslinked polyelectrolyte multilayer nanosurface and a terminal lipid layer that simultaneously tethers the cell membrane for improved spatial immobilization. Thermal imidization of the TetherChip nanosurface on commercially-available microfluidic slides allows up to 98% of tumor cell capture by the lipid tethers. Importantly, time-lapse microscopy demonstrates that unique microtentacles on non-adherent tumor cells are rapidly destroyed during chemical fixation, but tethering microtentacles to the TetherChip surface efficiently preserves microtentacle structure post-fixation and post-blood isolation. TetherChips remain stable for more than 6 months, enabling shipment to distant sites. The broad retention capability of TetherChips allows comparison of multiple tumor cell types, revealing for the first time that carcinomas beyond breast cancer form microtentacles in suspension. Direct integration of TetherChips into the Vortex VTX-1 CTC isolation instrument shows that live CTCs from blood samples are efficiently captured on TetherChips for rapid fixation and same-day immunofluorescence analysis. Highly efficient and unbiased label-free capture of CTCs on a surface that allows rapid chemical fixation also establishes a streamlined clinical workflow to stabilize patient tumor cell samples and minimize analytical variables. While current studies focus primarily on CTC enumeration, this microfluidic device provides a novel platform for functional phenotype testing in CTCs with the ultimate goal of identifying anti-metastatic, patient-specific therapies.

Received 2nd March 2020,
Accepted 26th June 2020

DOI: 10.1039/d0lc00207k

rsc.li/loc

Introduction

Tumor metastasis is the leading cause of cancer-associated mortality, yet it remains the most poorly understood component of cancer progression.[1] During metastasis, circulating tumor cells (CTCs) are shed from the primary tumor into the vasculature where they get transported to distant organs to seed and regrow. Studies have shown that CTCs serve as an early indicator of disease spread and survival in metastatic cancer patients.[2,3] However, CTCs are extremely rare cells (1 CTC per 1 billion blood cells in patients with advanced cancer) and are difficult to isolate and characterize, thus our understanding of their biological properties is limited.[4] Technical challenges of imaging non-adherent cells have led to the reliance on data generated solely from adherent cells, which is not necessarily predictive of treatment outcome. To overcome these obstacles, our lab

[a] *Marlene and Stewart Greenebaum NCI Comprehensive Cancer Center, University of Maryland School of Medicine, Bressler Research Building Rm 10-29, 655 W, Baltimore St., Baltimore, MD 21201, USA. E-mail: ssmartin@som.umaryland.edu; Tel: +410 706 6601*
[b] *Graduate Program in Molecular Medicine, University of Maryland School of Medicine, 800 W. Baltimore St., Baltimore, MD 21201, USA*
[c] *Department of Biochemistry and Molecular Biology, University of Maryland, Baltimore, 108 N. Greene Street, Baltimore, MD 21201, USA*
[d] *Department of Pharmacology and Physiology, University of Maryland School of Medicine, 655 W, Baltimore St., Baltimore, MD 21201, USA*
[e] *Fischell Department of Bioengineering, University of Maryland, College Park, 8228 Paint Branch Dr. College Park, MD 20742, USA*
[f] *United States Department of Veterans Affairs, VA Maryland Health Care System, USA*

† Electronic supplementary information (ESI) available. See DOI: 10.1039/d0lc00207k

‡ These authors contributed equally to the work.

has developed a microfluidic tethering platform, TetherChip, that recapitulates the free-floating microenvironment by preventing cell adhesion with a polyelectrolyte multilayer (PEM) nanosurface combined with a terminal lipid anchor to keep the suspended cells in place through interactions with the cell's lipid-based plasma membranes.[5] While tethered, cells also preserve their non-adherent cell behaviors, such as microtentacle (McTN) production.

Non-adherent cells display dramatically different cytoskeletal dynamics compared to cells adhered to an extracellular matrix (ECM).[6] Invadopodia are well-characterized, actin-based protrusions present on cells attached to the ECM that degrade the ECM through the local deposition of proteases to promote invasion.[7] In contrast, our lab discovered that non-adherent and circulating tumor cells produce long, microtubule-driven plasma membrane protrusions when detached from the ECM, known as microtentacles (McTNs), that result from changes in the actin-microtubule balance and are distinct from invadopodia.[8–10] McTNs are also distinct from cilia and flagella in their structure since doublets of microtubules support cilia and flagella, and recent electron microscopy studies demonstrate that McTNs contain exclusively singlet microtubules.[11] The number of microtubules within McTNs can range from several dozen in the thicker regions to just a few in the thinnest areas, but are not organized in any apparent way as they would be in an axoneme.[12] McTNs are enhanced in more aggressive tumor cells, promoting the reattachment of tumor cells to endothelial monolayers,[13] the formation of tumor cell clusters,[8,14] as well as increased retention of CTCs in the lungs of mice,[9,10] but are not observed when cells are grown on a matrix or solid culture surface, like glass or plastic. McTNs are thin, dynamic structures that are supported by the coordination of vimentin intermediate filaments and detyrosinated microtubules,[15] although recent evidence suggests that there is not an obvious direct interaction between the two filament types.[11] Electron microscopy illustrates that mature McTNs are well below 1 μm in diameter and taper gradually to below 100 nm at the distal ends.[11] This thinness potentially explains why McTNs may have been lost in earlier studies using chemical fixation. Additionally, it was recently indicated that septins localize at the base of McTNs and are required for their formation to promote attachment and cell–cell aggregation in detached tumor cells.[16] It is clear that non-adherent tumor cells possess significant molecular and functional differences than those grown on a flat surface or 3D matrix, therefore it is crucial to study CTCs in their native environment. The improved and optimized lipid tethering technology, TetherChip, described here provides a new opportunity to investigate CTC biology more in-depth and overcome the technical challenges of studying free-floating tumor cells.

Layer-by-layer (LBL) assembled polyelectrolyte multilayers (PEMs) are versatile nanostructured thin films that are used in a wide range of applications[17] and LBL deposition allows nanoscale control over thickness, composition, and molecular structure of the deposited film.[18] PEM films represent an attractive surface coating because they are ultra-thin, optically-clear, and cell-adhesion resistant.[18] We previously demonstrated that the deposition of four poly(methacrylic acid)/polyacrylamide (PMA/PAAm) bilayers showed the most reduced cell adhesion while maintaining McTN activity compared to 1 or 8 bilayers and that the addition of the lipid DOTAP (1,2-dioleoyl-3-trimethylammonium-propane), retained tumor cells more efficiently than the lipid DOPC (1,2-dioleoyl-*sn-glycero*-3-phosphocholine).[5] We also showed that the PEM+DOTAP tethering surface is nanometers-thin, with a single bilayer of PEM less than 10 nm thin, and 100% optically-clear, which is ideal for high-content and high-resolution imaging.[5] We observed that by formaldehyde crosslinking the DOTAP lipid tether to the PEM surface coating we could dramatically improve cell retention from 30% to almost 100% cell retention (manuscript in revision). However, the use of formaldehyde fixation to stabilize the PEM+DOTAP surface prevented the downstream use of formaldehyde to fix the tethered cells, since the reactive amines within the PEM had already been fully reacted during the initial formaldehyde step. Additionally, the high level of crosslinking that is achieved with formaldehyde greatly reduced the longevity of the tethering surface's adhesion-resistant properties. As a result, analysis using the previous iteration was limited to superficial membrane staining and a narrow time window for imaging. To overcome this, we sought to develop a method that would not only create a highly cytophobic surface that would maintain a near 100% cell retention with the DOTAP lipid tether but would also preserve the downstream ability to chemically fix tethered cells with a standard formaldehyde-based clinical fixative.

It was previously published that in aqueous buffers at a pH of 5 or higher, such as cell culture media, the multilayer films dissolve because of ionization of the carboxylic acid groups of PMA, leading to the disruption of the hydrogen-bonded network.[19] Thus, the stabilization of the PMA/PAAm layers is required to prevent the loss of the non-adherent tethering surface in culture. Yang *et al.* found that heating polyelectrolyte multilayer films introduced thermally-induced chemical crosslinks that stabilized the multilayer assembly even at pH 7 through a partial thermal imidization reaction, which produces imide crosslinks between the polymer bilayers.[20] The reaction temperature and time were optimized to allow for only a fraction of the polymers to crosslink; enough to prevent dissolution of the multilayer without changing its non-adherent properties. In a follow up study, this group went on to show that PMA/PAAm multilayers were found to exhibit a high resistance to cell adhesion, even with only a single bilayer coating.[18] Therefore, we hypothesized that thermal crosslinking a single PEM bilayer would be enough to stabilize the tethering surface and the subsequent addition of the DOTAP lipid layer would effectively retain suspended cells while preserving the ability to chemically fix cells for downstream analysis.

CTCs play an important role in metastasis formation and detection and analysis of CTCs obtained from the blood can potentially advance the diagnosis and treatment of cancer.[21] Liquid biopsies are minimally invasive and therefore provide real-time information and monitoring of a patient's cancer progression or recurrence. Over the past several years, countless techniques have been developed and utilized for CTC detection and isolation based on specific features of CTCs such as immunoaffinity with antibodies generally targeting either epithelial cell adhesion molecule (EpCAM) or cytokeratin (CK), or biophysical properties such as size, density, deformability or electric charge.[22] It has become increasingly evident however, that CTCs are a very heterogeneous population and do not always express EpCAM and/or CK, leading to the development of label-free isolation techniques that do not require immunorecognition and now allow for the recovery of viable cells, such as ANGLE's Parsortix, Celsee's Celselect Genesis system, CROSS chip and Vortex's VTX-1 as well as many others.[23–29] The Parsortix, Genesis and CROSS chip systems all capture CTCs directly on each of their microfluidics chips and require an extra step to be able to harvest the CTCs to a different vessel, such as TetherChip, with either an inverted flow or using a microcapillary tool.[25–28] The VTX-1 however, allowed TetherChip to be directly placed at the output of the CTC isolation chip.[29] As discussed above, microtentacles are very thin and fragile structures, therefore rapid isolation systems that do not require extensive pre-processing steps and minimal sample manipulation are preferred when studying these structures. Although all of these enrichment strategies pose various advantages and limitations (extensively reviewed in[22,24]) and are still fully compatible with TetherChip, we ultimately prioritized the Vortex VTX-1 platform in this study due to its quick isolation processing time, minimal cell manipulation as well as ease of directly harvesting viable cells onto the TetherChip for downstream analysis.

In this study, we optimize and improve the stability of the TetherChip to allow for downstream fixation of non-adherent cells and increased functionality for CTC analysis. By replacing our lipid formaldehyde crosslinking step with a partial thermal imidization crosslinking reaction on the nanometer-thin PEM deposited onto Ibidi microfluidic slides, we extend the applications of this technology with the proven capabilities of cell capture, crosslinked stabilization, wash tolerance, and archival tumor cell fixation. We found that thermal imidization of the PEM created a stable surface that rapidly captured up to 98% of seeded cells with the lipid tethers while also maintaining a cytophobic surface for at least 48 hours. For the first time, we demonstrate the ability to formaldehyde fix tethered cells without destroying McTN morphology and structure. We further validate the robustness of the device by defining optimal parameters for complete cell capture as well as McTN retention. Additionally, we expand the applications of the tethering surface to include the top four cancers by incidence (breast, lung, prostate, and colon) and illustrate for the first time McTN production of these cell lines in suspension. Enhanced tethering capabilities of the technology allow us to directly integrate our device into various CTC isolation platforms to confidently capture rare cells from liquid biopsy samples.

Materials and methods

Cell lines and materials

MDA-MB-436 and MCF-7 cell lines were purchased from ATCC and cultured with Dulbecco's modified Eagle medium (DMEM, Corning) supplemented with 10% fetal bovine serum (Atlanta Biologicals) and 1% penicillin–streptomycin (Gemini) solution. MDA-MB-231TD (tumor-derived) cells were produced in our lab (manuscript in submission) and cultured as described above. MDA-MB-231 GFP and luciferase stably expressing cells were inoculated into mice and allowed to grow for approximately 35 days. The tumors were resected, homogenized and the collected cells were used for experiments. SNU-C1, H1755, H1944, H2087 cell lines were purchased from ATCC and cultured with Roswell Park Memorial Institute (RPMI, Corning) media supplemented with 10% fetal bovine serum and 1% penicillin–streptomycin. PC-3 and LNCaP cell lines were cultured with RPMI media supplemented with 10% fetal bovine serum and 1% penicillin–streptomycin. T84 cells were purchased from ATCC and cultured with DMEM/F12 media supplemented with 5% fetal bovine serum and 1% penicillin–streptomycin. Cells were maintained in a humidified environment at 37 °C and 5% CO_2. Poly(methacrylic acid) (PMA, MW = 100 000, Cat: 00578) and polyacrylamide (PAAm, MW = 5 000 000–6 000 000, Cat: 02806-50) were purchased from Polysciences. Poly(allylamine hydrochloride) (PAH, MW ~ 200 000, Cat: 43092) was purchased from Alfa Aesar. 1,2-Dioleoyl-3-trimethylammonium-propane(chloride salt) (DOTAP) was purchased from Avanti Polar Lipids (Cat: 890890C). The PEM–DOTAP nanosurface was deposited onto uncoated Ibidi microfluidic channel slides (μ-Slide VI 0.4 or μ-Slide I Luer 0.8) in all experiments. NucBlue Live ReadyProbes Reagent (Invitrogen) was used to stain the nucleus for all live cell experiments and Hoechst 33258 was used to stain the nucleus for all fixed experiments.

Polyelectrolyte multilayer (PEM) and lipid film deposition

For multilayer film deposition, similar to methods previously published,[5,18] Poly(allylamine hydrochloride) (PAH) was prepared as a 0.05 M solution using ultrapure water and adjusted to pH 3.0 using 10 M hydrochloric acid. Poly(methacrylic acid) (PMA) and polyacrylamide (PAAm) were prepared as 0.01 M solutions using ultrapure water and adjusted to pH 3.0 using 10 M hydrochloric acid. All polymer solutions were filtered with a 0.45 μm cellulose nitrate filter prior to use in multilayer film assembly. Uncoated microfluidic slides (μ-Slide VI 0.4) (Ibidi) were coated first with 120 μL of polycationic solution (PAH) (0.05 M) for 15 minutes to introduce a primer/adhesion layer, then rinsed twice for 1 minute each using deionized (DI) water adjusted

to pH 3.0 with 10 M hydrochloric acid. The primer layer was followed by the addition of 120 μL of polyanionic PMA (0.01 M) for 5 minutes and rinsed twice for 1 minute each with pH 3.0 DI water. Then, 120 μL of nonionic PAAm (0.01 M) was deposited and rinsed as described above. For additional bilayers, the process was repeated without the addition of the priming layer (PAH) until the desired number of bilayers was assembled. DOTAP lipid was prepared as a 0.001 M solution in pH 3.0 deionized water and sonicated for 60 minutes in a room temperature water bath. After sonication, 100 μL of lipid solution was added to the microchannel for 5 minutes followed by two rinse steps. To thermally crosslink, microfluidic slides were placed in an oven at 90 °C for 8 hours under a vacuum before the addition of the lipid. For the slides that were prepared using the traditional formaldehyde-crosslinking, 120 μL of a 3.7% formaldehyde solution diluted in phosphate-buffered saline (PBS) was added to the microfluidic channels, after the addition of DOTAP, for 5 minutes followed by two rinse steps. Following deposition, slides were allowed to air dry for 1 hour at room temperature before use. For experiments using Ibidi μ-Slide I Luer 0.8 channel slides (cell suspension assay and VTX-1 isolation experiments), slides were coated with 300 μL of all PEM reagents and 200 μL of DOTAP lipid to cover the larger surface area of these vessels. A single bilayer of PEM + DOTAP is termed $(PMA/PAAm)_1$ + DOTAP and four bilayers is $(PMA/PAAm)_4$ + DOTAP throughout the paper.

Tethering wash tolerance

MDA-MB-436, MDA-MB-231TD, and MCF-7 cells (5000 cells/channel) were trypsinized and stained with NucBlue Live ReadyProbes Reagent (Invitrogen) then seeded on microfluidic slides coated with either thermal-crosslinked $(PMA/PAAm)_1$ + DOTAP or formaldehyde-crosslinked $(PMA/PAAm)_4$ + DOTAP (Ibidi, μ-Slide VI 0.4). Cells were incubated for 30 minutes at 37 °C, unless otherwise stated, to allow for tethering. To quantify initial cell number, whole channel scans in the DAPI channel were taken for each condition using the Nikon Eclipse Ti2-E inverted microscope at 4× magnification. After 30 minutes, 100 μL of PBS was washed through the top port of the microfluidic channel and 75 μL was gently removed at the bottom port. This was considered one wash. All washes or reagent additions were performed in this manner (100 μL in, 75 μL out) for all experiments throughout this study unless otherwise stated. Following each wash, whole channel scans were again taken for each condition as described above. The cell number after each wash was quantified using NIS Elements software and normalized to the initial cell number to calculate percent cell retention.

Cell suspension assay

MDA-MB-436, MDA-MB-231TD, and MCF-7 cells (200 cells/channel) were trypsinized and seeded on either thermal-crosslinked $(PMA/PAAm)_1$ + DOTAP or formaldehyde-crosslinked $(PMA/PAAm)_4$ + DOTAP microfluidic slides (Ibidi, μ-Slide I Luer 0.8). Cells were incubated for 30 minutes at 37 °C to allow for tethering and an initial whole channel scan (time = 0) in brightfield was taken for each condition using the Nikon Eclipse Ti2-E inverted microscope at 10× magnification. Additional whole channel scans were done at each indicated time point for each condition. The number of cells that were still tethered (not spread/adhered on the surface) at each time point was counted and normalized to the initial number of tethered cells at $t = 0$ to calculate the percent of cells that remained tethered and non-adherent during the time course.

McTN counting

MDA-MB-231TD and MDA-MB-436 cells were trypsinized and resuspended in phenol red-free and serum-free DMEM. Cells (50 000 cells/channel) were seeded on thermal-crosslinked $(PMA/PAAm)_1$ + DOTAP coated microfluidic slides (Ibidi, μ-Slide VI 0.4). Cells were incubated for 30 minutes to allow for tethering. For live McTN counts, after 30 minutes one wash was done where 100 μL of fresh media was added to the top port of the microfluidic slides and 75 μL was gently removed from the bottom port. This wash was to ensure only tethered cells were analyzed. After this wash, CellMask Orange (Life Technologies) cell membrane dye was added to each channel at a final concentration of 1 : 10 000. For fixed McTN counts, after 30 minutes 3.7% formaldehyde/PBS was washed through each channel to fix cells for 10 minutes. Wheat germ agglutinin (WGA, Alexa Fluor 594 Conjugate, Invitrogen) was then added to each channel at a final concentration of 1 : 100 to visualize the cell membrane. McTNs were scored in a population of 100 cells/channel as previously described.[8]

Immunofluorescence

MDA-MB-436 cells were allowed to tether for 30 minutes onto $(PMA/PAAm)_1$ + DOTAP coated microfluidic slides (Ibidi, μ-Slide VI 0.4) then fixed with 3.7% formaldehyde/PBS, washed, permeabilized in 0.1% Triton-X 100/PBS, blocked in 5% bovine serum albumin (BSA)/PBS, and incubated overnight at 4 °C in 5% BSA/PBS with an antibody against α-tubulin (Sigma-Aldrich, Cat: T6199) at the manufacturer recommended dilution. Secondary antibodies, anti-mouse Alexa Fluor 488 (Thermo Fisher, 1 : 5000), WGA (Alexa Fluor 594 conjugate, Invitrogen, 1 : 100), and Hoechst 33258 (1 : 5000) were diluted in BSA/PBS, added to each channel, and incubated for 2 hours at room temperature. Images were acquired using an Olympus IX81 microscope with a Fluoview FV1000 confocal laser scanning system.

McTN image analysis on fixation time points

MDA-MB-436 and MDA-MB-231TD cells were trypsinized and seeded onto thermal-crosslinked $(PMA/PAAm)_1$ + DOTAP coated microfluidic slides (Ibidi, μ-Slide VI 0.4). Cells were incubated for various time points (0, 1, 5, 15, 30, 45, or 60 minutes) before fixation with 3.7% formaldehyde for 10 minutes. After 10 minutes, Hoechst 33258 (1 : 5000) and WGA

(Alexa Fluor 594 Conjugate, Invitrogen, 1 : 100) were added to each channel. Images were acquired using an Olympus IX81 microscope with a Fluoview FV1000 confocal laser scanning system. Perimeter quantification was done in ImageJ as shown in Fig. S4B.†

Spiked CTC isolation using the VTX-1 and tethering

The VTX-1 device was operated using the procedures as previously described.[29] MDA-MB-231TD (10^2) cells were spiked into 4 mL of whole blood diluted in PBS to a total volume of 40 mL, for a 10× blood dilution. Cells were immediately tethered post-isolation for 45 minutes, as the output of the VTX-1 (200 μl total volume) was directly collected into an Ibidi microfluidic slide coated with thermal-crosslinked $(PMA/PAAm)_1$ + DOTAP capable of retaining 300 μL total volume (Ibidi, μ-Slide I Luer 0.8) (see Fig. 6). After processing, cells were fixed with 300 μL 3.7% formaldehyde and stained with 300 μL of Hoechst 33258 (1 : 5000) to visualize the nucleus and WGA (Alexa Fluor 594 Conjugate,

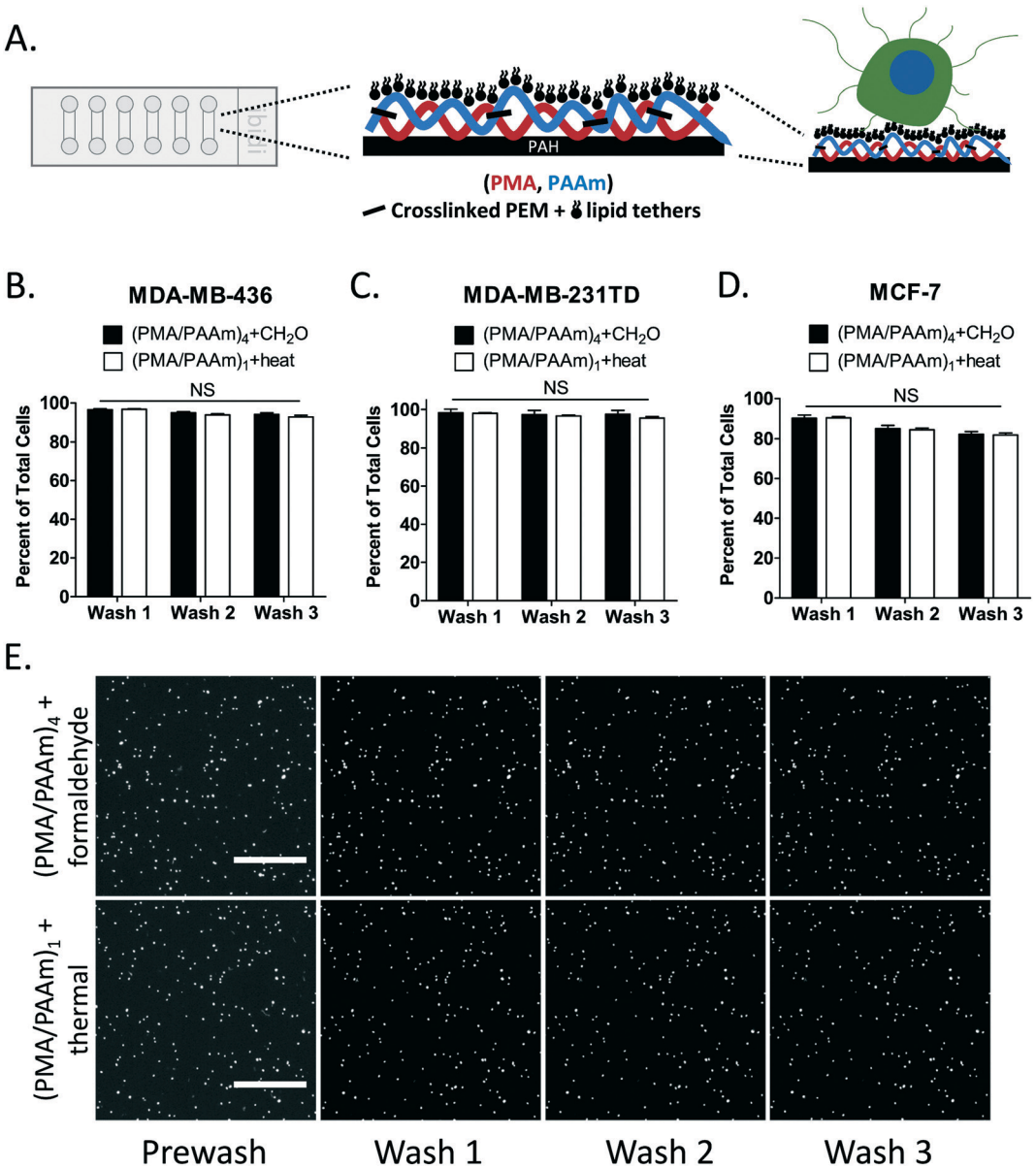

Fig. 1 Thermal-crosslinking of PEM+DOTAP has similar cell retention to formaldehyde crosslinking DOTAP to PEM. A) Diagram of improved tethering surface with 1 bilayer and the addition of thermal crosslinking. B–D. Percent of tethered cell retention after sequentially washing B) MDA-MB-436, C) MDA-MB-231TD and D) MCF7 cells on microfluidic slides coated with $(PMA/PAAm)_4$+DOTAP with formaldehyde (CH_2O)-crosslink or thermal-crosslinked $(PMA/PAAm)_1$+DOTAP (heat). Data are shown as mean ± SEM, n = 3; NS, $P > 0.05$ *vs.* $(PMA/PAAm)_1$+heat (two-way ANOVA with Bonferroni posttest). E) Representative images of tethered MDA-MB-436 cells stained with NucBlue Live ReadyProbes Reagent on $(PMA/PAAm)_4$+DOTAP with formaldehyde-crosslink and $(PMA/PAAm)_1$+DOTAP with thermal-crosslink microfluidic slides after washing. Images were taken at 4× magnification in the DAPI channel on the Nikon Eclipse Ti2-E inverted microscope. Scale bar = 500 μm.

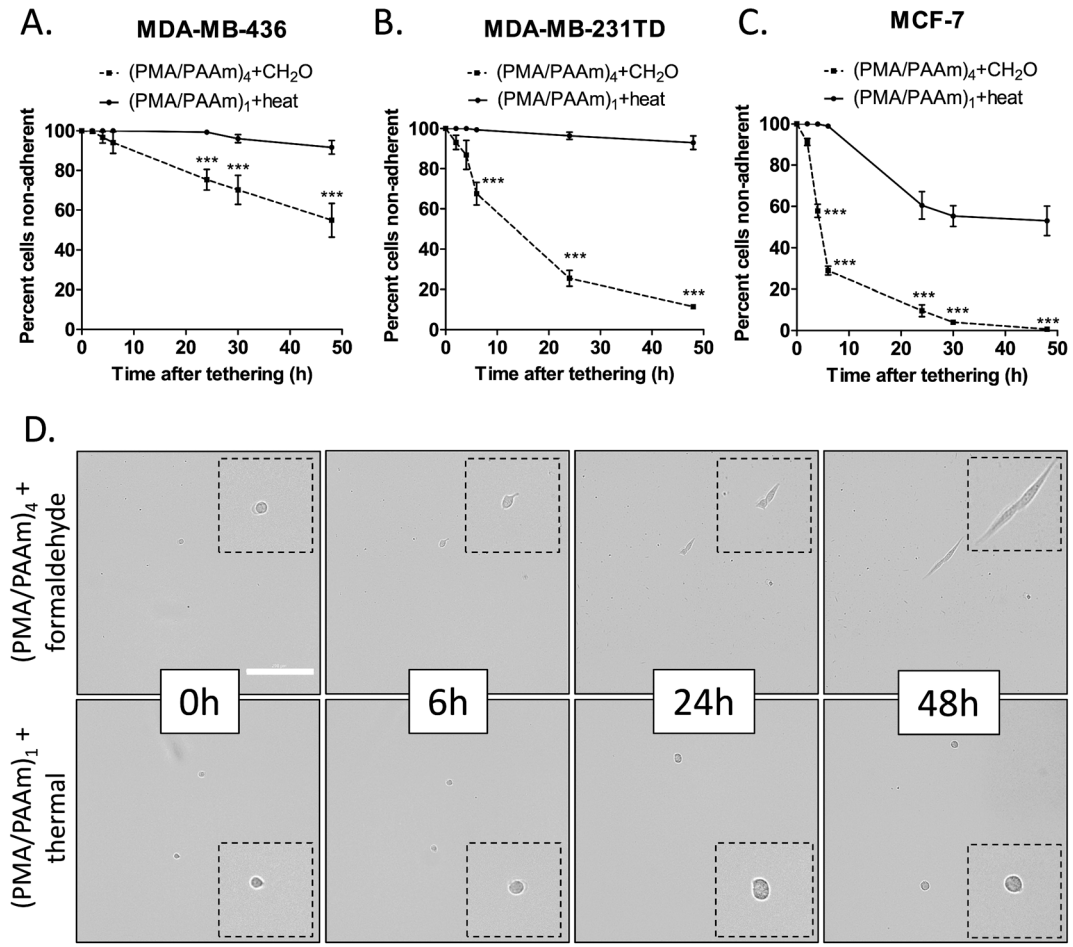

Fig. 2 Thermal-crosslinking of PEM+DOTAP prolongs cell suspension on tethering surface. A–C. Percent of A) MDA-MB-436, B) MDA-MB-231TD and C) MCF-7 cells on microfluidic slides coated with $(PMA/PAAm)_4$+DOTAP with formaldehyde-crosslink (CH_2O) or thermal-crosslinked $(PMA/PAAm)_1$+DOTAP (heat) that have remained rounded without adhesion/spreading after the indicated time points. Data are shown as mean ± SEM, $n = 3$; ***, $P < 0.001$ *vs.* $(PMA/PAAm)_1$+thermal (two-way ANOVA with Bonferroni posttest). D) Representative brightfield images of tethered MDA-MB-436 cells on $(PMA/PAAm)_4$+DOTAP with formaldehyde-crosslink and thermal-crosslinked $(PMA/PAAm)_1$+DOTAP coated microfluidic slides after indicated time points. Brightfield images were taken at 10× magnification on the Nikon Eclipse Ti2-E inverted microscope. Scale bar = 200 μm.

Invitrogen, 1 : 100) to visualize the cell membrane. Images were acquired using an Olympus IX81 microscope with a Fluoview FV1000 confocal laser scanning system.

Desiccator experiments

Slides were coated with thermal-crosslinked $(PMA/PAAm)_1$ + DOTAP (Ibidi, μ-Slide VI 0.4) and either placed on the benchtop in ambient conditions or in a glass desiccator containing silica gel (Acros Organics, Cat: 7631-86-9). Slides were removed at each month for 6 months for each condition simultaneously to test capture efficiency. MDA-MB-436 and MDA-MB-231TD cells were seeded onto either a slide stored in ambient conditions or in the desiccator and were incubated for 30 minutes at 37 °C to allow for tethering. Each channel was washed three times, as described above in "Tethering Wash Tolerance". The cell number after each wash was quantified using NIS Elements software and normalized to the initial cell number to calculate percent cell retention.

Statistical analysis

GraphPad Prism (version 6.02) was used to determine all statistical comparisons. One-way and two-way ANOVA tests were performed with a Bonferroni multiple comparisons post-test as indicated. A *p*-value of 0.05 or less was considered statistically significant.

Results and discussion

Thermal-crosslinking of PEM plus DOTAP improves cell retention

Live tumor cells can be tethered to surfaces engineered with PEM+DOTAP, but are not well-retained during routine washing procedures that are required for many laboratory procedures (only 10–40% cells retained after 3 washes).[5] We

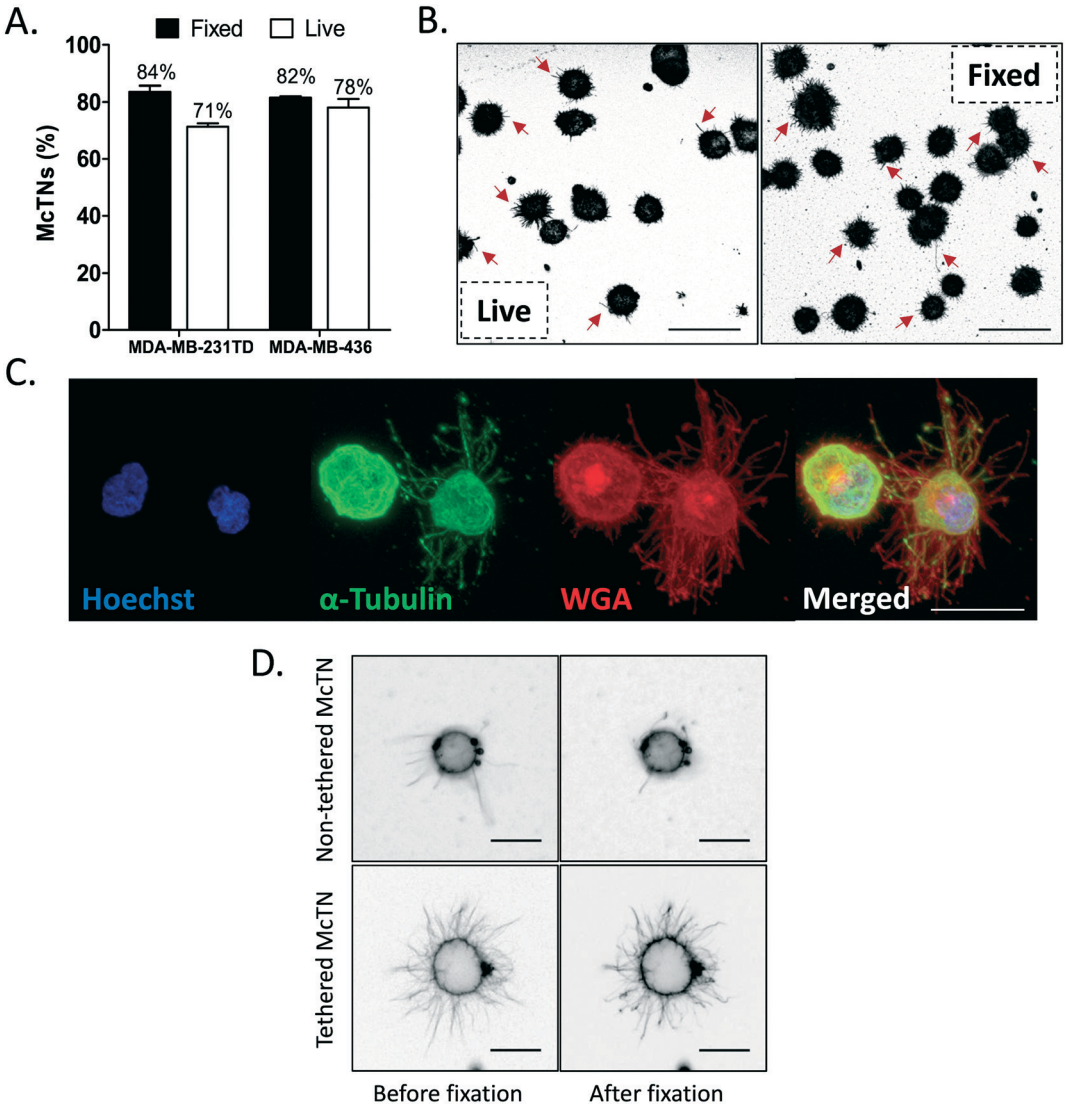

Fig. 3 Thermal-crosslinking of PEM+DOTAP enables fixation of microtentacles. A) Live *versus* fixed McTN quantification of MDA-MB-436 cells tethered on microfluidic slides coated with thermal-crosslinked $(PMA/PAAm)_1$+DOTAP. Data represents quantification of McTN frequency from three independent experiments with 100 cells counted for each (mean ± SEM). B) Representative images of live MDA-MB-436 cells stained with CellMask Orange (1 : 10 000, left panel) or fixed cells stained with WGA (wheat germ agglutinin, Invitrogen, 1 : 100, right panel). Scale bar = 50 μm. C) Immunofluorescent images of tethered and fixed MDA-MB-436 cells stained with Hoechst 33258 (1 : 5000, blue), α-tubulin (1 : 1000, green), and WGA (wheat germ agglutinin, 1 : 100, red) were taken at 60× magnification using an Olympus IX81 microscope with a Fluoview FV1000 confocal laser scanning system. Scale bar = 20 μm. D) Representative still frames of tethered MDA-MB-436 cells with McTNs that are free-floating (top panel) or tethered to the lipid surface (bottom panel), pre- and post-fixation. Videos were taken either immediately after cell tethering (non-tethered McTN, 5 minutes) or 30 minutes after tethering to allow McTN to tether to the lipid surface. Brightfield images were taken at 20× magnification on the Nikon Eclipse Ti2-E inverted microscope. Scale bar = 20 μm.

decided to compare two crosslinking methods (thermal imidization and formaldehyde reaction) to improve the cell retention durability of PEM+DOTAP nanosurfaces. Earlier observations in our lab have shown that formaldehyde treatment of 4 bilayers of polymethacrylic acid and polyacrylamide (PMA/PAAm) can improve cell retention compared to uncrosslinked surfaces (manuscript under revision), but do not maintain cytophobic properties over long periods of time. Given observations that thermal crosslinking of a single polyelectrolyte bilayer yields a surface that greatly resists cell adhesion,[18] we decided to measure whether thermal crosslinking of a single PMA/PAAm bilayer could serve as an improved PEM foundation for the cell tethering technology that might also retain the downstream capability of formaldehyde cell fixation. Breast cancer cells were seeded onto microfluidic slides coated with $(PMA/PAAm)_4$+DOTAP with formaldehyde crosslink or thermal-crosslinked $(PMA/PAAm)_1$+DOTAP (Fig. 1A) and their initial retention and wash tolerance rates were measured. During successive wash steps, the thermal-crosslinked $(PMA/PAAm)_1$+DOTAP coating retained cells at a similar rate to slides coated with $(PMA/PAAm)_4$+DOTAP with formaldehyde

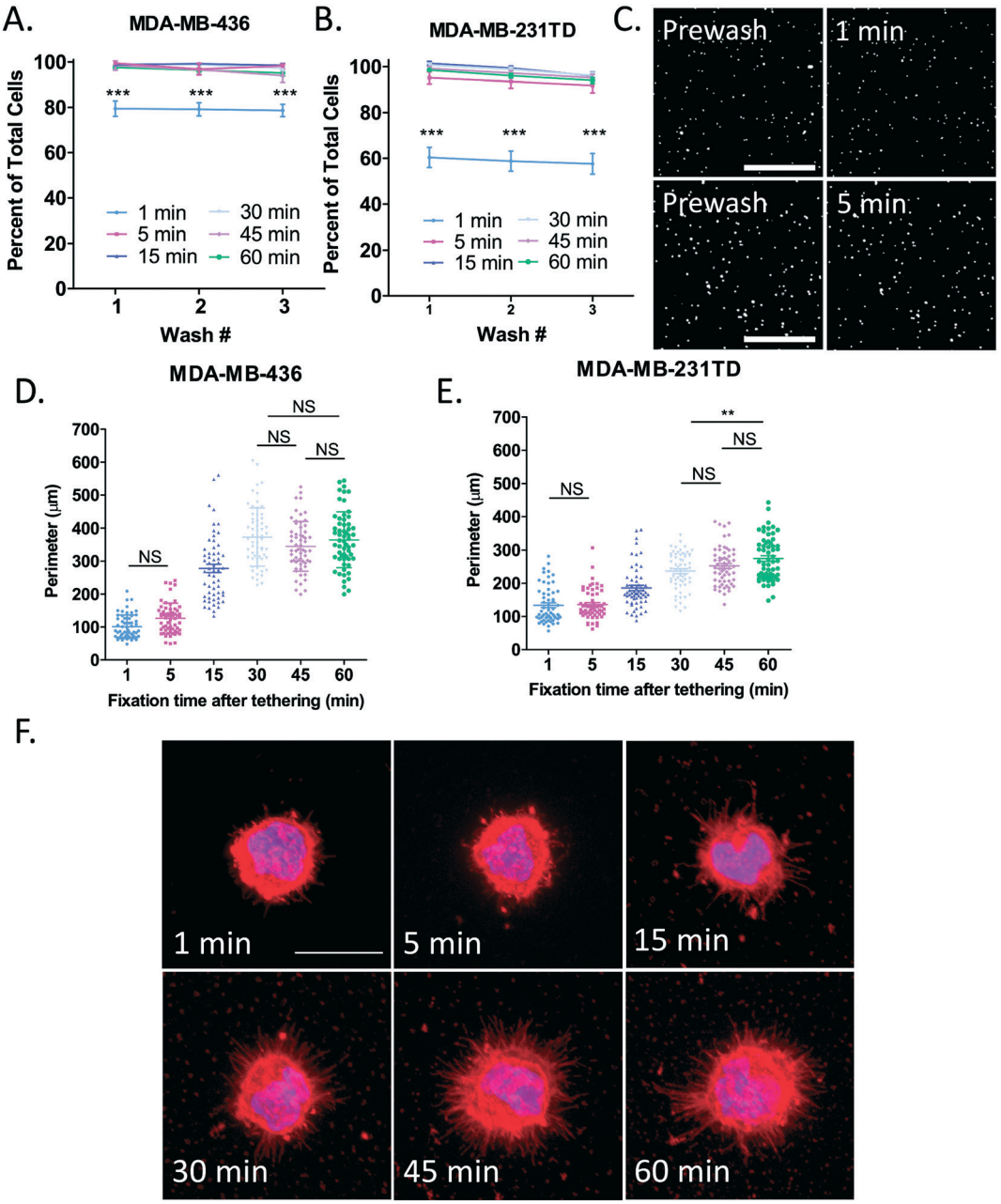

Fig. 4 Time course of cell tethering and microtentacle fixation on thermal-crosslinked surface. A and B. Percent of tethered cell retention after sequentially washing A) MDA-MB-436 or B) MDA-MB-231TD cells on microfluidic slides coated with thermal-crosslinked $(PMA/PAAm)_1$+DOTAP after the indicated time points. Data are shown as mean ± SEM, $n = 3$; ***, $P < 0.001$ *vs.* 1 minute (two-way ANOVA with Bonferroni posttest). C) Representative images of tethered MDA-MB-436 cells stained with NucBlue Live ReadyProbes Reagent on microfluidic slides coated with thermal-crosslinked $(PMA/PAAm)_1$+DOTAP either washing after 1 minute (top panel) of tethering time or 5 minutes (bottom panel). Images were taken at 4× magnification in the DAPI channel on the Nikon Eclipse Ti2-E inverted microscope. Scale bar = 500 μm. D and E) Quantification of the perimeter of either D) MDA-MB-436 cells or E) MDA-MB-231TD cells at each of the indicated time points analyzed by ImageJ. Data are shown as mean ± SEM, $n = 3$; all multiple comparisons are significant with $P < 0.001$ unless otherwise stated on graph; **, $P < 0.01$; NS, $P > 0.05$ *vs.* indicated data point (one-way ANOVA with Bonferroni posttest). F) Representative images of tethered MDA-MB-436 cells fixed at either 1, 5,15, 30, 45, or 60 min post-tethering and stained with Hoechst 33258 (1 : 5000) and WGA (1 : 100). Images were taken at 60× magnification using an Olympus IX81 microscope with a Fluoview FV1000 confocal laser scanning system. Scale bar = 20 μm.

crosslink over all three wash steps for MDA-MB-436 (Fig. 1B), MDA-MB-231TD (Fig. 1C) and MCF-7 (Fig. 1D) cell lines. For both tethering surfaces, 97% of MDA-MB-436 cells, 98% of MDA-MB-231TD cells and 90% of MCF-7 cells were retained after the first wash. Even after three washes MDA-MB-436 and MDA-MB231TD cells continued to maintain 95% of the initially tethered cells, while MCF-7 cells retained over 80%. Representative images over three washes show minimal cell loss when cells are tethered with either method of crosslinking (Fig. 1E and S1A†). These results demonstrate

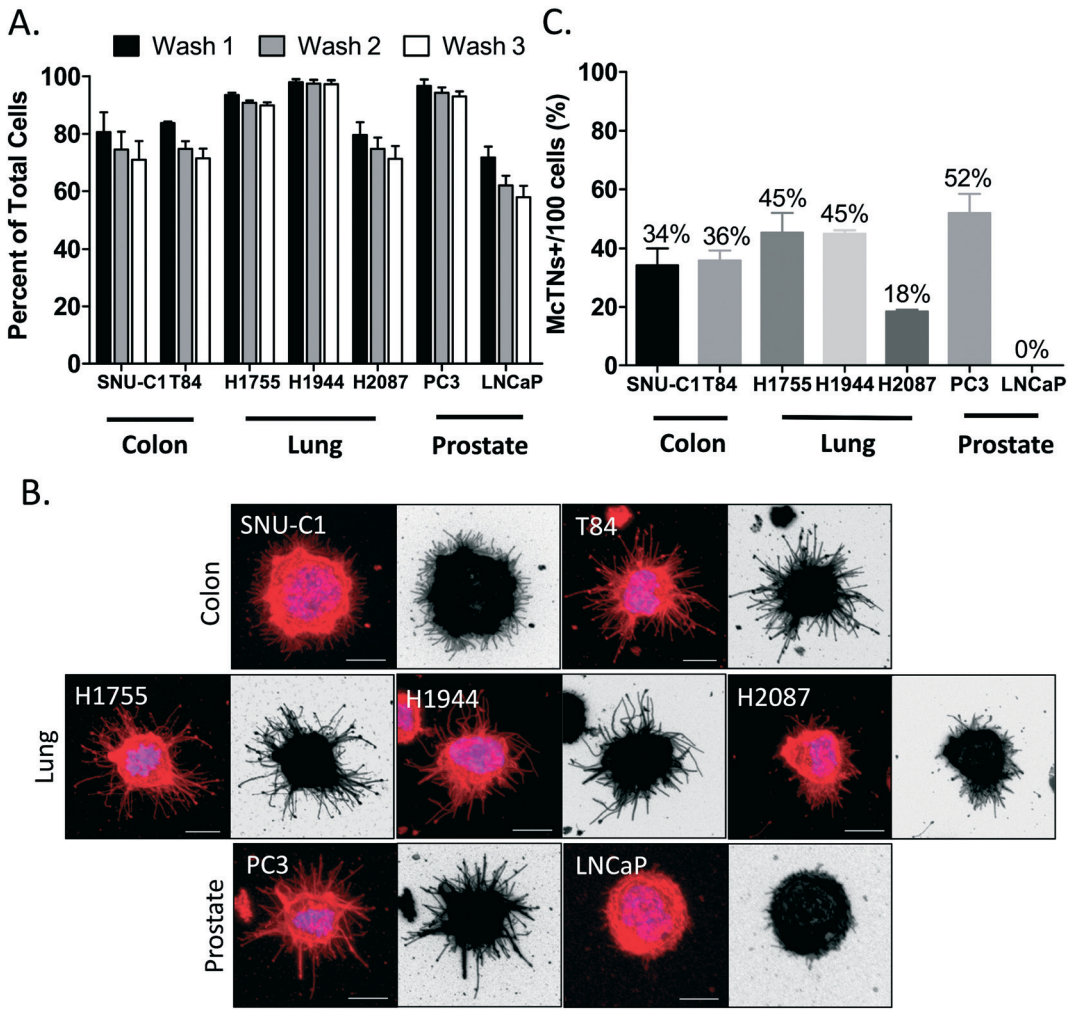

Fig. 5 Thermal-crosslinking of PEM+DOTAP also retains colon, lung and prostate cancer cell lines. A) Percent of tethered cell retention after sequentially washing colon, lung, and prostate cancer cell lines on microfluidic slides coated with thermal-crosslinked $(PMA/PAAm)_1$+DOTAP. Data represents wash tolerance from three independent experiments (mean ± SEM). B) Representative images of each cancer cell line that was tethered, fix and stained with Hoechst 33258 (1 : 5000) and WGA (1 : 100) (left panel) and the same image inverted (right panel) to better visualize McTN formation. Images were taken at 60× magnification using an Olympus IX81 microscope with a Fluoview FV1000 confocal laser scanning system. Scale bar = 10 μm. C) Fixed McTN quantification of each cancer cell line tethered on microfluidic slides coated with thermal-crosslinked $(PMA/PAAm)_1$+DOTAP. Data represents quantification of McTN frequency from three independent experiments with 100 cells counted for each (mean ± SEM).

that crosslinked tethering surfaces maintain a very high retention efficiency for different cell lines during multiple wash steps.

The concept of studying non-adherent cells with a microfluidic device, such as TetherChip, has become extremely important given the recent advances in elucidating the mechanisms of CTC metastasis, such as the process of epithelial-to-mesenchymal transition (EMT) and its reverse process, mesenchymal-to-epithelial transition (MET). It has been proposed that primary tumor cells activate EMT to invade and disseminate through the body, and upon arriving at the distant sites they undergo MET to form epithelial metastasis.[30] A better understanding of how these processes are regulated will lead to therapeutic targets for metastasis prevention, however it is important that these studies occur in an environment that most closely recapitulates the blood stream (non-adherent conditions) where dissemination can occur. Highly efficient cell retention in a microfluidic device to perform these types of experiments is crucial for the analysis of extremely rare cells, like CTCs. These results confirm that thermal-crosslinking does achieve a high level of initial cell retention and subsequent wash tolerance retention, which is similar to the formaldehyde-crosslinked surface. It is also worth noting that because the crosslinked tethering surfaces retain cells after multiple washes, this enables the capability to add dyes or drugs or perform washing steps without displacing the non-adherent, tethered cells. Because of these improvements in surface chemistry to yield a cell retention rate of 98%, we can be confident moving forward in performing experiments where CTC number may be very low, such as in patient-derived xenografts (PDX) or patient blood samples. We also show

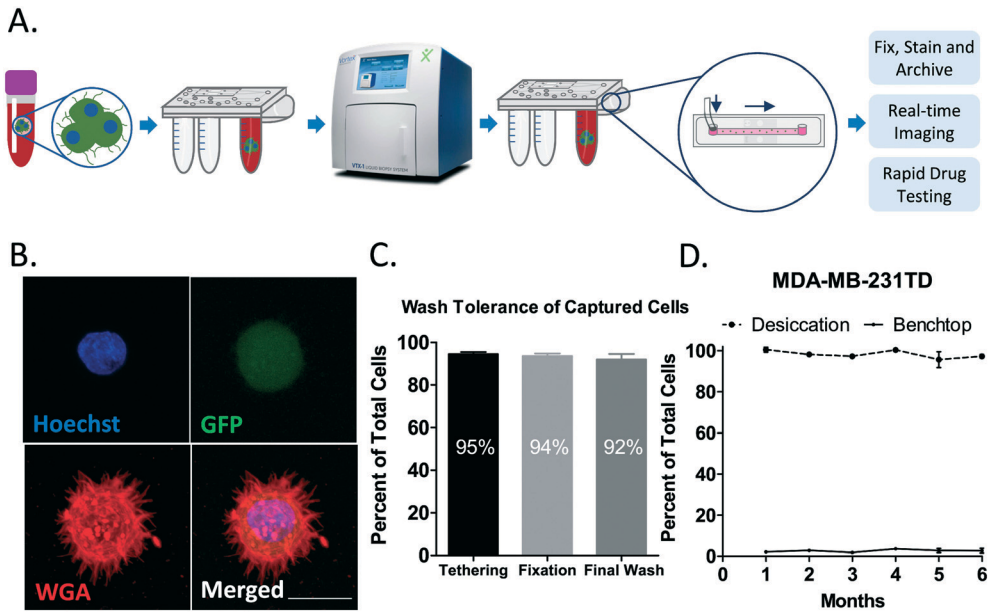

Fig. 6 Efficient tethering of CTCs recovered from blood samples and device shelf-life. A) Diagram of the process of CTC isolation in Vortex's VTX-1 with a direct output onto TetherChips, which allows for downstream analysis of suspended cells. B) Representative image of MDA-MB-231TD cells that were spiked into whole blood, isolated in the VTX-1, tethered onto a TetherChip surface (thermal-crosslinked $(PMA/PAAm)_1$+DOTAP) and then fixed and stained with Hoechst 33258 (1 : 5000) and WGA (1 : 100). Images were taken at 60× magnification using an Olympus IX81 microscope with a Fluoview FV1000 confocal laser scanning system. Scale bar = 20 μm. C) Percent of cell retention after tethering, fixing and staining of MDA-MB-231TD cells that were spiked into whole blood, isolated in the VTX-1, and delivered to a TetherChip surface. Data are shown as mean ± SEM. D) Percent of tethered cell retention after sequentially washing MDA-MB-231TD cells on TetherChips that had been stored in a glass desiccator or on the benchtop for the indicated time points. Data are shown as mean ± SEM, n = 1 with triplicates.

here that the sample preparation for utilizing TetherChip is relatively easy compared to other devices, without the need for any prior enrichment such as EpCAM staining, therefore it can capture all CTCs regardless of whether they have undergone EMT or not. Given the nanometer-thin and optically-clear surface features of TetherChip for high-resolution imaging as well as the enhanced initial cell retention and wash tolerance capabilities to securely hold free-floating cells in place, this microfluidic device has already proven to be instrumental in overcoming technical challenges of studying non-adherent tumor cells.

Thermal-crosslinked tethering surface prolongs cell suspension

Besides a high cell tethering efficiency, a nanoscale tethering surface that resists cell adhesion would improve the ability to study cell behaviors that occur in the non-adherent microenvironments that are encountered during metastasis through the bloodstream or lymphatics. To test how cells would interact with the two differentially crosslinked surfaces over longer periods of time, the same three breast cancer cell lines were seeded onto microfluidic slides coated with $(PMA/PAAm)_4$+DOTAP (formaldehyde-crosslink) or $(PMA/PAAm)_1$+DOTAP (thermal-crosslink) for a 48 hour time course. For all three cell lines MDA-MB-436 (Fig. 2A), MDA-MB-231TD (Fig. 2B) and MCF-7 (Fig. 2C), the thermal-crosslinked tethering surface significantly reduced cell adhesion compared to the formaldehyde-crosslinked surface as early as 4 hours after seeding. Representative images of the same cell at each of the indicated time points up to 48 hours illustrate that the thermal-crosslinked PEM exerts a much higher level of cell adhesion resistance than the formaldehyde-crosslinked film especially 6 hours after seeding (Fig. 2D and S2A†). MCF-7 cells are highly adherent and begin attaching to the formaldehyde-crosslinked surfaces within 2 hours. Thermal-crosslinked surfaces resist MCF-7 adhesion for at least 10 hours, and these cells do eventually attach by 24 hours, but still significantly less than on formaldehyde-crosslinked surfaces (Fig. 2C). These results illustrate that the thermal-crosslinked surface prevents cell adhesion and spreading to a much greater degree than the formaldehyde-crosslinked surface, prioritizing thermal crosslinking as the main method of stabilization for maintaining a non-adherent microenvironment.

Thermal imidization at 90 °C for 8 hours produces a small fraction of imide bonds (about 1% of the acid/amide groups get converted into imide bonds) that stabilize the film for at least one month even in the typical buffered solutions used in most cell culture assays.[18] Typically, PMA/PAAm films become soluble at a pH higher than 5.0 and therefore dissolve in neutral buffered solutions due to ionization of the PAAm acid groups disrupting the hydrogen-bonded network and introducing electrostatic repulsive forces.[20] Low levels of crosslinking allow polyelectrolyte multilayers to swell and act as a hydrogel so the cells are not able to recognize it as a

mechanically supportive surface for adhesion.[18] Since formaldehyde at pH 7 crosslinks the multilayers to a much greater degree, it is possible that reduced multilayer swelling provides a surface that allows eventual cell adhesion. These results verified that the thermal-crosslinked tethering surface was not only able to maintain free-floating tumor cell characteristics (by preventing attachment and cell spreading), but also kept cells tethered (held securely by the lipid while maintaining non-adherent behaviors) for that time period to allow for tracking while prohibiting cell aggregation. Ultimately, this provides the ability to accurately track individual cells in the whole slide over at least 2 days, for assays such as sphere formation or drug response where it is impossible to do this with traditional low-attach plates because of cell drift. Having the ability to track individual cells opens the opportunity to differentiate single cells in a heterogenous mixture especially when analyzing drug response. Minimizing the drift of non-adherent cells with lipid tethers could also reduce cell clustering artifacts that typically confound traditional sphere-forming assays.[31] Additionally, utilizing the thermal-crosslinked surface provides a potential application for longer term measurements of non-adherent cell responses such as anoikis, or death by detachment from extracellular matrix, and stem cell sphere formation. Anoikis experiments occur over a time scale of between 8 h and 24 h depending on cell type and traditional stem cell sphere formation assays continue for 7–14 days. Because the formaldehyde-crosslinked surface only resists cell adhesion for a maximum of 3–4 hours, these longer assays would not be feasible. On the other hand, thermal-crosslinked PEM surfaces can remain cell-adhesion resistant in culture for up to one month.[18] The ability to tether and track individual cells over long periods of time enables the opportunity to perform phenotypic experiments that would have otherwise been impractical for non-adherent cells.

Thermal-crosslinked tethering surface enables microtentacles to be formaldehyde fixed

Since thermal crosslinking only converts a small fraction of reactive acid/amine groups to imide bonds,[18] it is possible that the residual unreacted amine groups could be exploited to chemically fix the tumor cells and microtentacles to the tethering surface with formaldehyde. Our previous studies have shown that microtentacles on live, free-floating tumor cells collapse during formaldehyde fixation, presumably due to the inability of the free-floating microtentacles to form crosslinks with a stabilizing surface and the delicate microtentacle structure, which electron microscopy reveals can be less than 100 nm in diameter.[11] This collapse of free-floating microtentacles during fixation is most clearly evident with time-lapse microscopy during fixation (Video S1†). To determine if thermal-crosslinked PEM+DOTAP nanosurfaces could enable more efficient McTN fixation, McTN frequency was assessed with either free-floating, live tumor cells or tumor cells that had been first tethered and then fixed with formaldehyde. McTN counts in both MDA-MB-436 and MDA-MB-231TD cells revealed only a small difference in frequency between the live *versus* fixed cells for both cell lines (Fig. 3A). In both cell types, fixation actually increased the levels of cells scoring positive for McTNs by a blinded observer (Fig. 3A). We believe fixation does not necessarily alter McTN frequency, but instead improves visualization by capturing McTNs onto the single focal plane of the tethering surface. In live samples, McTNs extend across many focal planes and move dynamically, complicating the ability to visualize all McTNs in live tumor cells. In fixed samples, we allowed cells to tether for at least 30 minutes before fixation, which allowed the McTNs to also lay down onto a single focal plane and tether to the lipid surface. Because these McTNs were no longer free-floating and were bound to a surface, they were able to survive chemical fixation. Representative images of live and fixed MDA-MB-436 (Fig. 3B) and MDA-MB-231TD (Fig. S3A†) cells demonstrate a high McTN frequency in both conditions. To further validate that cells and their McTNs could be fixed without changing composition or phenotype, immunofluorescent staining was performed for α-tubulin and the plasma membrane. Consistent with previous publications from the lab,[8,15,32] immunofluorescence revealed microtubules extend along the length of McTNs (Fig. 3C). These results not only show that downstream fixation is possible with a thermal-crosslinked tethering surface, but it also shows that this surface is robust enough to withstand the continuous washing involved in immunofluorescent staining. Chemical fixation also revealed strong heterogeneity in McTN phenotype between cells from the same tumor cell line (Fig. 3C), which we have shown is linked to both differences in stem cell characteristics[33] and epithelial-to-mesenchymal transition (EMT) markers.[13] While observing McTN behavior, it was noticed that some cells had free-floating McTNs and some had McTNs that had laid down and tethered to the lipid surface. To determine the difference between these two states in terms of fixation potential, time-lapse videos during the initial formaldehyde addition were taken of a MDA-MB-436 cell with non-tethered McTNs (Video S1†) and another with tethered McTNs (Video S2†). Representative still frames of these videos show that during the initial formaldehyde fixation, the non-tethered, free-floating McTNs collapse and largely disappear after only about 20 seconds post-formaldehyde wash while the tethered McTNs remain intact (Fig. 3D). These results display that McTNs which are allowed to tether to the lipid have the ability to be fixed without being completely destroyed. We concluded that this difference in tethered *versus* non-tethered McTNs was the result of how long the cells and their McTNs were allowed to tether undisturbed before fixation. Therefore, in order to obtain a reproducible method for fixation and be able to further archive samples of tethered cells, we decided to move forward by optimizing the tethering time that allows McTNs to engage the lipid surface for maximum preservation during chemical fixation.

Recent electron microscopy studies have shown that McTNs are very thin, flexible structures with diameters ranging from 100 nm to 1 μm and lengths of tens of micrometers.[11] Our results demonstrate that McTNs are extremely sensitive to fixation, which in combination with the thinness, could be one reason McTNs have been largely overlooked in previous studies. We show that immediately after formaldehyde is washed through the channel, the untethered McTNs already begin to collapse (Video S1†). On free-floating surfaces such as low-attach plates, especially after a longer fixation time such as the standard 10 minute formaldehyde fixation, the McTNs would be strongly reduced. By integrating the lipid, which indiscriminately binds plasma membrane, the cell body along with the McTNs are able to be tethered. We illustrate that the tethering of the McTNs actually protects them from collapse during fixation, which permits immunofluorescent staining as well as other downstream applications. Additionally, by using a thermal imidization reaction to stabilize the PEM surface instead of a chemical crosslink, such as formaldehyde, the reactive amine groups are still available for the fixation of tethered cells to the surface for immunofluorescence and eventual archival storage. Lipophilic dyes, such as CellMask Orange, which we have used in our previous studies to visualize McTNs in live cells, also bind to the lipid tethering surface which creates a significant amount of background fluorescence. Additionally, CellMask does not survive permeabilization and therefore cannot be used for immunofluorescence procedures. This led us to prioritize wheat germ agglutinin (WGA), which is a general glycosylation binding protein and is amenable to permeabilization and thus immunofluorescence. WGA stains a broad variety of cell types in an antibody-independent manner, allowing both our cell tethering mechanism and our staining protocol to work across many tumor types creating a universal protocol. The novel fixation capability of TetherChip adds to its simple sample preparation, where cells seeded onto the microfluidic device do not have to be manipulated any further for image analysis and archival. Rapid chemical fixation will help preserve samples, especially with patient CTCs that are exceptionally rare in blood samples. Variables introduced during extended processing of live patient tumor cells in clinical labs can also be minimized through rapid chemical fixation and generate an archival sample that can be stored for years. Additionally, by stabilizing the cell morphology and phenotype the sample can be transported from clinical sites for research and analysis without the use of incubators or dry ice. Additionally, this unique surface chemistry of TetherChip allows for high-resolution imaging and easy detection due to the innovative focal plane restriction of McTNs and the advanced ability to perform immunofluorescence staining on McTNs. Given these practical advantages of the thermal-crosslinked PEM+DOTAP nanosurface (TetherChip), we prioritized this formulation for additional studies.

Time course of cell tethering and McTN fixation on tethering surface

Before determining the length of time McTNs need to lay down onto the tethering surface to most easily visualize them, it first had to be established exactly how long it took for cells to become completely tethered. To do this, MDA-MB-436 (Fig. 4A) and MDA-MB-231TD (Fig. 4B) cells were seeded onto microfluidic slides coated with thermal-crosslinked PEM+DOTAP and allowed to tether for either 1, 5, 15, 30, 45 or 60 minutes. In both cell lines, TetherChips robustly captured cells within only 5 minutes of tethering even after 3 consecutive washes. Representative images of tethered MDA-MB-436 cells illustrate that even only after 1 minute of cell tethering to thermal-crosslinked PEM+DOTAP surfaces, there is already almost an 80% cell retention rate with MDA-MB-436 cells, but at 5 minutes nearly 100% of the cells are tethered (Fig. 4A and C). Since TetherChips are able to capture cells within just 5 minutes, we next determined the timeframe of McTN tethering to help define a standard protocol for tumor cell fixation that maximizes McTN preservation. Quantification of cell perimeter (Fig. S4B†) as a simple measurement of McTN presence (a larger perimeter would correlate with more McTNs) shows the largest change in the perimeter for MDA-MB-436 cells (Fig. 4D) between 5 and 15 minutes of tethering and between 15 and 30 minutes for MDA-MB-231TD cells (Fig. 4E). For both cell lines the perimeter continues to increase for 30 minutes and then begins to level off between 45–60 minutes post-tethering. Multiple comparison tests reveal a significant difference ($p < 0.001$) between each time point shown unless stated otherwise on the graphs. Representative images from each time point illustrate the progression of McTN formation and tolerance to fixation over the course of 1 hour for MDA-MB-436 (Fig. 4F) and MDA-MB-231TD (Fig. S4A†). It is clear that after 1 and 5 minutes of tethering, McTNs have not begun to lay down onto the lipid tethering surface yet and are consequently damaged by the fixation. It has been shown that at 3 minutes McTNs begin to form and by 5 minutes they are well-developed,[11] therefore by 5 minutes we should see be able to see McTNs and their absence in the fixed samples indicates McTNs were likely destroyed by the fixation. These results display that the tethering technology is able to fully retain cells within 5 minutes of seeding, but because McTNs need at least 30 minutes to bind to the lipid tethers and plateau by 45 minutes, we implemented a standard 45-minute tethering time for moving forward with fixation studies. This is the first time we have quantified and optimized tethering time for the TetherChip device, but by developing these standardized procedures we take TetherChip one step further in the process of commercialization.

Although we demonstrate above that more MDA-MB-231TD cells are positive for McTNs than MDA-MB-436 cells (Fig. 3A), we establish here that MDA-MB-436 cells seem to have more or longer McTNs as shown by a larger overall

perimeter (Fig. 4D and E). Both of these cell types are known to be aggressive and metastatic, but it brings up an interesting question of whether the number of cells producing McTNs (whether long or short) or the length of each McTN is more crucial for reattachment. We know from previous publications from our lab that McTNs promote reattachment to endothelial cells,[33] but the mechanism by which they do this is still unknown. It is also known that tumor cell heterogeneity plays a major role in metastasis, drug resistance, and clinical outcome.[34] Even within the same cell type, we demonstrate that cells can possess very different phenotypes with either very long McTNs or almost none at all (Fig. 3C). Along with those observations, we also see some variation in perimeter within each cell line and at the various time points (Fig. 4D and E). TetherChip provides the potential to track individual tethered cells to see which ones can resist different chemotherapies and which cells can develop into large spheres over time (implicating a stem-like phenotype), while also demonstrating which cells undergo anoikis or do not survive drug treatments.

Tethering surface also retains colon, lung and prostate cancer cell lines

In addition to breast cancer cells, we also expand the application potential of TetherChip technology to include lung, prostate and colon cancer cells. In 2018, these were the top four cancers (including breast) by incidence and accounted for almost half of all cancers.[35] SNU-C1, T84, NCI-H1755, NCI-1944, NCI-2087, PC-3 and LNCaP cancer cells were seeded onto TetherChips and the tethering efficiency was analyzed over three subsequent washes. H1755, H1944 and PC-3 cells all tethered with a greater than 90% cell retention over all washes while SNU-C1, T84 and H2087 cells tethered with about an 80% retention (Fig. 5A). LNCaP prostate cancer cells did not tether well and only about half remained after the three washes. Although some of these other cancer cell lines do not tether as well as breast cancer cells, a 70% retention rate (after three washes) is still sufficient to conduct preliminary downstream analysis for cell lines where the number of cells is abundant. Additionally, the methodology could be optimized for different cell lines where differences in phenotypes (Fig. S5 and Table S1†) or membrane lipid compositions may affect tethering efficiency. Besides examining whether other types of cancer cells could be tethered, we were also interested in determining if these other cell lines also produced McTNs in suspension. Representative images of tethered cells illustrate that lung, prostate and colon cancer cells do indeed produce McTNs with varying lengths and degree of frequency (Fig. 5B). Quantification of McTN frequency demonstrates that even within cancer types, different cell lines produced McTNs at varying rates (Fig. 5C). The largest differences were observed in the prostate cancer cell lines, PC-3 (grade IV) and LNCaP (stage D1), which were on complete opposite ends of the McTN spectrum with 52% *versus* 0%, respectively, which is consistent with their tumorigenicity and metastatic capacity *in vivo*.[36] Lung cancer cell lines, H1755 and H1944, had a comparable McTN frequency while H2087 exhibited considerably less McTNs, which also parallels the aggressiveness of these cell lines (stage 4, stage 3b, and stage 1, respectively). Colon cancer lines, SNU-C1 and T84, also had a similar rate of McTNs, with T84 being slightly higher. T84 cells have been shown to be tumorigenic[37] and mildly metastatic[38] *in vivo* while SNU-C1 cells have not been reported to be tumorigenic,[39] potentially further extending the correlation between McTNs and aggressiveness. We show here, for the first time, that this tethering technology indiscriminately captures these four major tumor cell types, as well as illustrates that McTN formation is shared amongst many cell lines when put into suspension, potentially associated with metastatic potential.

About 90% of all solid human tumors originate in epithelial tissues as carcinomas,[40] with a positive correlation between incidence and age.[41] The top four cancers by incidence (lung, colorectal, breast, prostate) are each predominantly epithelial in origin and account for almost half of all cancers. By expanding the applicability of the TetherChip to be able to tether several different cancer types, we can begin to analyze metastatic phenotypes (McTNs, stem cell sphere formation, clustering) from these cancers as well. We highlight here that the TetherChip lipid surface indiscriminately holds multiple cell types without bias from antibody/surface markers or attachment/matrix receptors. Improvements in the TetherChip technology made it possible to illustrate for the very first time that McTNs do exist in other epithelial tumor cell types. This novel biological finding suggests that McTNs could be a common phenotype of carcinomas, given their presence in these top four human solid tumor types. Additionally, we have previously shown that McTNs are an indicator of tumor stem cell characteristics,[33] epithelial-to-mesenchymal transition (EMT),[13] and loss of the PTEN tumor suppressor,[14] which further supports our current demonstration of a potential correlation between number of McTNs and aggressiveness of the tumor cell type.[15] McTNs might therefore, be an indicator of tumorigenic potential (growth) as well as metastatic potential (reattachment and clustering).

TetherChips allow for efficient tethering of CTCs recovered from blood samples

Development of a platform to study cells in a free-floating state that can be directly integrated into established CTC isolation technologies provides an efficient and valuable tool to investigate the behaviors of circulating tumor cells with minimal manipulation. Live CTCs can be isolated, with an instrument such as the Vortex VTX-1, with a direct output of 200 μL total volume onto a TetherChip, which can then be fixed and stained for further downstream analysis as well as archived for later use (Fig. 6A). This relatively new concept of recovering cells *via* the Vortex straight onto TetherChip shows

the potential of this microfluidic device in its capability of being directly integrated into any kind of enrichment platform for CTC isolation. Importantly, there are currently many systems in development for the isolation of CTCs, but there are very few options post-isolation for CTC analysis. Fig. 6B is a representative image of a MDA-MB-231TD cell that was spiked into 4 mL of whole blood, isolated on the VTX-1 machine, tethered and then fixed and stained. This is the type of image that can be acquired within 1 hour post-isolation and further analyzed. The ability of a direct output onto a tethering slide with 95% tethering efficiency and a retention rate of 98% once the cells have been fixed (Fig. 6C) means that utilizing this platform for clinical samples, where number is often limited, is very feasible and highly reliable. However, it is important to note that these blood isolation experiments were performed with cells expressing GFP as a proof-of-concept that allowed positive identification of tumor cells and robust determination of the TetherChip retention efficiency. For clinical sample analysis, it will be necessary to combine CTC enrichment from systems like the VTX-1 with immunostaining on the TetherChip that can identify tumor cells (CK/EpCAM) and exclude contaminating lymphocytes (CD45), since the GFP confirmation is not possible. With this established, rapid workflow, the TetherChip offers a complete ready-to-use, Lab-on-a-Chip solution for non-adherent cell image analysis that overcomes challenges associated with cell drift when imaging free-floating cells, cell displacement when washing drugs or dyes through, and avoids long-term culture by measuring drug effects on McTNs from single cells. For TetherChips to be a truly ready to use product, we also needed to verify a reasonable shelf-life. We previously noticed that in ambient conditions on the benchtop, the TetherChips would only last about a week before the lipid started to degrade, and cells would not tether anymore. To test whether we could extend this, we seeded MDA-MB-436 cells and MDA-MB-231TD cells onto the thermal-crosslinked microfluidic slides that had either been on the benchtop in ambient conditions or in a glass desiccator for the indicated time points and their retention rates were measured after 3 consecutive washes. For both MDA-MB-231TD (Fig. 6D) and MDA-MB-436 (Fig. S6A†) cells, the slide stored in the desiccator was able to retain about 97% of the total initially seeded cells as compared to about a 4% retention rate for the slide that was not stored in a desiccator. We demonstrate here that not only do TetherChips currently have at least a 6 month shelf life, but they are most importantly an easy-to-use, plug and play platform for the analysis and archival storage of circulating tumor cells with multiple potential applications to study metastatic phenotypes.

Current systems to analyze patient tumor cells such as patient-derived xenografts (PDX) and other long-term culture systems such as spheroids, can impose selective and adaptive pressures to tumor cells. These pressures usually result in either cells failing to grow or the tumor cells that eventually do grow are not entirely representative of the original sample. Additionally, these models take weeks to months for implementation and are not guaranteed to work. TetherChip analysis, on the other hand, can be completed within hours of isolation from the patient, minimizing uncontrolled variables and offering an immediate conclusion, avoiding the complications of long-term growth. Further, the compatibility of thermal-crosslinking with downstream chemical cell fixation also reduces variables in this process to more tightly streamline a clinical workflow and produce a consistently archived sample. We have proven that with the TetherChip, CTCs can be spatially immobilized and therefore imaged in high-resolution and McTNs can be objectively measured with an automated software[42] for responses to chemotherapy drugs such as taxol and colchicine in less than one hour. With the nanoscale surfaces on TetherChip that provide maximal optical clarity, we can easily employ this platform for high-content and high-resolution imaging. Utilizing this technology offers the possibility to not only be able to rapidly study non-adherent cell behavior, but also to target metastatic phenotypes like McTNs that only are present when cells are in suspension. Most tumor assessments are still being conducted by analyzing growth and how growth changes in response to drug treatments. Emerging evidence however, has demonstrated that chemotherapies like paclitaxel that reduce tumor size in breast cancer, actually promote McTNs,[43] CTC shedding, and increases in metastasis.[44] Technologies like the TetherChip open the opportunity to measure metastatic phenotypes independent of growth and therefore possibly identify new therapies that are specific to metastasis and do not necessary affect growth. While current cancer therapies target microtubules indiscriminately,[6] the dependence of McTNs on detyrosinated subsets of microtubules may offer opportunities to specifically target detyrosination[45] and therefore reduce off-target side effects of broadly inhibiting cell growth. The recent identification of the long-elusive tubulin carboxypeptidase may also present a potential therapeutic target for selective McTN targeting.[46,47] Metastatic phenotypes such as McTN formation, CTC clusters, and stem cell sphere formation only occur in a non-adherent, free-floating state, as adherent and non-adherent cells possess dramatically different functional and molecular characteristics. TetherChip can provide fundamental insights into these non-adherent, single-cell behaviors of metastatic tumor cells that could improve the therapeutic targeting of metastasis and overcome the limiting focus of exclusively targeting tumor growth for patient monitoring and cancer drug development.

Conclusions

In this study, we develop an improved and more stabilized lipid tethering system using thermal imidization that enables rapid chemical fixation of non-adherent tumor cells in a free-floating environment with the ability to preserve microtentacle structure post-fixation and post-blood isolation (Fig. 3 and 6). By thermal-crosslinking only a small percentage of the PEM nanosurface, cells can be tethered

with up to a 98% retention rate and remain non-adherent (but still tethered) for at least 48 hours (Fig. 1 and 2). Further, we demonstrate for the first time, that colon, lung, and prostate cancer cells can not only be tethered, but that they also produce McTNs when in suspension, which positively correlates to cell line aggressiveness (Fig. 5). Directly integrating this tethering technology with new isolation technologies that allow the capture of live CTCs, such as the Vortex VTX-1, now establishes that it is both possible and feasible to conduct McTN analysis on a small number of isolated CTCs within only a few hours and without requiring tumor cell propagation (Fig. 6). A major advantage of the ability to fix the cells directly to the tethering slide is the stabilization of cell morphology and phenotype, which not only enables high-content imaging, but also the option to transport these slides between clinical and research sites. Taken together, this study establishes a microfluidic cell tethering platform (TetherChip) to analyze metastatic phenotypes in a wide range of tumor cell types with a streamlined workflow that is feasible for precision medicine applications with the small numbers of tumor cells available from patient biopsies or blood samples.

Author contributions

Conceptualization and design: J. A. J., C. J. L., C. M. J. and S. S. M.; acquisition of data: J. A. J. and C. J. L.; analysis and interpretation: J. A. J., C. J. L., K. N. T., E. C. O., R. M. L., T. J. M., S. J. P. P., M. I. V., C. M. J., and S. S. M.; manuscript draft: J. A. J.; manuscript edits: J. A. J., C. J. L., K. N. T., E. C. O., R. M. L., T. J. M., S. J. P. P., M. I. V., C. M. J., and S. S. M. All authors read and approved the final manuscript.

Conflicts of interest

The University of Maryland own patents on the subject of microtentacles and microfluidic cell tethering that list two of the authors on the current manuscript (Christopher M. Jewell and Stuart S. Martin) as inventors. Christopher M. Jewell and Stuart S. Martin are employees of the VA Maryland Health Care System. The views reported in this paper do not reflect the views of the Department of Veterans Affairs or the United States Government.

Acknowledgements

We thank Vortex Biosciences and ANGLE plc for collaborating on this study. This work was supported in part by the METAvivor Foundation and grants from the National Institutes of Health to SSM (R01-CA154624, R01-CA124704) and CMJ (R01-EB027143) as well as the Veterans Administration to SSM (I01-BX002746) and CMJ (I01-BX003690). MIV was supported by (122229-IRG-97-153-10-IRG, RSG-18-028-01-CSM) from the American Cancer Society and (K01CA166575) from the National Cancer Institute. ECO was supported by (133192-PF-19-017-01-CSM) from the American Cancer Society and (5T32CA154274-07) from the National Cancer Institute. SJPP was supported by grants from the National Cancer Institute (5T32GM008181-30, 1F31CA232393-01). The Greenebaum Comprehensive Cancer Center is supported by P30-CA134274 and the Maryland Cigarette Restitution Fund.

References

1 C. L. Chaffer and R. A. Weinberg, A perspective on cancer cell metastasis, *Science*, 2011, **331**, 1559–1564, DOI: 10.1126/science.1203543.
2 M. Cristofanilli, Circulating tumor cells, disease progression, and survival in metastatic breast cancer, *Semin. Oncol.*, 2006, **33**, S9–S14, DOI: 10.1053/j.seminoncol.2006.03.016.
3 B. Rack, *et al.* Circulating tumor cells predict survival in early average-to-high risk breast cancer patients, *J. Natl. Cancer Inst.*, 2014, **106**(5), DOI: 10.1093/jnci/dju066.
4 M. Yu, S. Stott, M. Toner, S. Maheswaran and D. A. Haber, Circulating tumor cells: approaches to isolation and characterization, *J. Cell Biol.*, 2011, **192**, 373–382, DOI: 10.1083/jcb.201010021.
5 K. R. Chakrabarti, *et al.* Lipid tethering of breast tumor cells enables real-time imaging of free-floating cell dynamics and drug response, *Oncotarget*, 2016, **7**, 10486–10497, DOI: 10.18632/oncotarget.7251.
6 K. R. Chakrabarti, L. Hessler, L. Bhandary and S. S. Martin, Molecular Pathways: New Signaling Considerations When Targeting Cytoskeletal Balance to Reduce Tumor Growth, *Clin. Cancer Res.*, 2015, **21**, 5209–5214, DOI: 10.1158/1078-0432.CCR-15-0328.
7 R. Buccione, J. D. Orth and M. A. McNiven, Foot and mouth: podosomes, invadopodia and circular dorsal ruffles, *Nat. Rev. Mol. Cell Biol.*, 2004, **5**, 647–657, DOI: 10.1038/nrm1436.
8 R. A. Whipple, A. M. Cheung and S. S. Martin, Detyrosinated microtubule protrusions in suspended mammary epithelial cells promote reattachment, *Exp. Cell Res.*, 2007, **313**, 1326–1336, DOI: 10.1016/j.yexcr.2007.02.001.
9 M. A. Matrone, *et al.* Metastatic breast tumors express increased tau, which promotes microtentacle formation and the reattachment of detached breast tumor cells, *Oncogene*, 2010, **29**, 3217–3227, DOI: 10.1038/onc.2010.68.
10 E. M. Balzer, *et al.* c-Src differentially regulates the functions of microtentacles and invadopodia, *Oncogene*, 2010, **29**, 6402–6408, DOI: 10.1038/onc.2010.360.
11 A. N. Killilea, *et al.* Cytoskeletal organization in microtentacles, *Exp. Cell Res.*, 2017, **357**, 291–298, DOI: 10.1016/j.yexcr.2017.05.024.
12 I. R. Gibbons, Cilia and flagella of eukaryotes, *J. Cell Biol.*, 1981, **91**, 107s–124s, DOI: 10.1083/jcb.91.3.107s.
13 R. A. Whipple, *et al.* Epithelial-to-mesenchymal transition promotes tubulin detyrosination and microtentacles that enhance endothelial engagement, *Cancer Res.*, 2010, **70**, 8127–8137, DOI: 10.1158/0008-5472.CAN-09-4613.
14 M. I. Vitolo, *et al.* Loss of PTEN induces microtentacles through PI3K-independent activation of cofilin, *Oncogene*, 2013, **32**, 2200–2210, DOI: 10.1038/onc.2012.234.

15 R. A. Whipple, *et al.* Vimentin Filaments Support Extension of Tubulin-Based Microtentacles in Detached Breast Tumor Cells, *Cancer Res.*, 2008, **68**, 5678–5688, DOI: 10.1158/0008-5472.can-07-6589.

16 K. Ostevold, *et al.* Septin remodeling is essential for the formation of cell membrane protrusions (microtentacles) in detached tumor cells, *Oncotarget*, 2017, **8**, 76686–76698, DOI: 10.18632/oncotarget.20805.

17 G. Decher, Fuzzy Nanoassemblies: Toward Layered Polymeric Multicomposites, *Science*, 1997, **277**, 1232–1237, DOI: 10.1126/science.277.5330.1232.

18 S. Y. Yang, J. D. Mendelsohn and M. F. Rubner, New class of ultrathin, highly cell-adhesion-resistant polyelectrolyte multilayers with micropatterning capabilities, *Biomacromolecules*, 2003, **4**, 987–994, DOI: 10.1021/bm034035d.

19 S. A. Sukhishvili and S. Granick, Layered, Erasable, Ultrathin Polymer Films, *J. Am. Chem. Soc.*, 2000, **122**, 9550–9551, DOI: 10.1021/ja002410t.

20 S. Y. Yang and M. F. Rubner, Micropatterning of polymer thin films with pH-sensitive and cross-linkable hydrogen-bonded polyelectrolyte multilayers, *J. Am. Chem. Soc.*, 2002, **124**, 2100–2101.

21 E. Racila, *et al.* Detection and characterization of carcinoma cells in the blood, *Proc. Natl. Acad. Sci. U. S. A.*, 1998, **95**, 4589–4594, DOI: 10.1073/pnas.95.8.4589.

22 M. M. Ferreira, V. C. Ramani and S. S. Jeffrey, Circulating tumor cell technologies, *Mol. Oncol.*, 2016, **10**, 374–394, DOI: 10.1016/j.molonc.2016.01.007.

23 S. D. Mikolajczyk, *et al.* Detection of EpCAM-Negative and Cytokeratin-Negative Circulating Tumor Cells in Peripheral Blood, *J. Oncol.*, 2011, **2011**, 252361, DOI: 10.1155/2011/252361.

24 H. Cho, *et al.* Microfluidic technologies for circulating tumor cell isolation, *Analyst*, 2018, **143**, 2936–2970, DOI: 10.1039/c7an01979c.

25 L. Xu, *et al.* Optimization and Evaluation of a Novel Size Based Circulating Tumor Cell Isolation System, *PLoS One*, 2015, **10**, e0138032, DOI: 10.1371/journal.pone.0138032.

26 R. Riahi, *et al.* A novel microchannel-based device to capture and analyze circulating tumor cells (CTCs) of breast cancer, *Int. J. Oncol.*, 2014, **44**, 1870–1878, DOI: 10.3892/ijo.2014.2353.

27 P. Gogoi, *et al.* Development of an Automated and Sensitive Microfluidic Device for Capturing and Characterizing Circulating Tumor Cells (CTCs) from Clinical Blood Samples, *PLoS One*, 2016, **11**, e0147400, DOI: 10.1371/journal.pone.0147400.

28 S. Ribeiro-Samy, *et al.*Fast and efficient microfluidic cell filter for isolation of circulating tumor cells from unprocessed whole blood of colorectal cancer patients, *Sci. Rep.*, 2019, **9**, 8032, DOI: 10.1038/s41598-019-44401-1.

29 E. Sollier, *et al.* Size-selective collection of circulating tumor cells using Vortex technology, *Lab Chip*, 2014, **14**, 63–77, DOI: 10.1039/C3LC50689D.

30 J. P. Thiery, Epithelial-mesenchymal transitions in tumour progression, *Nat. Rev. Cancer*, 2002, **2**, 442–454, DOI: 10.1038/nrc822.

31 P. C. Bailey, *et al.* Single-Cell Tracking of Breast Cancer Cells Enables Prediction of Sphere Formation from Early Cell Divisions, *iScience*, 2018, **8**, 29–39, DOI: 10.1016/j.isci.2018.08.015.

32 A. E. Boggs, *et al.* α-Tubulin Acetylation Elevated in Metastatic and Basal-like Breast Cancer Cells Promotes Microtentacle Formation, Adhesion, and Invasive Migration, *Cancer Res.*, 2015, **75**, 203–215, DOI: 10.1158/0008-5472.can-13-3563.

33 M. S. Charpentier, *et al.* Curcumin targets breast cancer stem-like cells with microtentacles that persist in mammospheres and promote reattachment, *Cancer Res.*, 2014, **74**, 1250–1260, DOI: 10.1158/0008-5472.CAN-13-1778.

34 L. Schnipper, Clinical implications of tumor-cell heterogeneity, *N. Engl. J. Med.*, 1986, **314**, 1423–1431, DOI: 10.1056/NEJM198605293142206.

35 J. Ferlsay, M. Ervik, F. Lam, M. Colombet, L. Mery, M. Piñeros, A. Znaor, I. Soerjomataram and F. Bray, *Global Cancer Observatory: Cancer Today*, 2018, https://gco.iarc.fr/today.

36 S. Tai, *et al.* PC3 is a cell line characteristic of prostatic small cell carcinoma, *Prostate*, 2011, **71**, 1668–1679, DOI: 10.1002/pros.21383.

37 A. W. Baird, D. H. Miller, D. A. Schwartz and H. S. Margolius, Enhancement of kallikrein production and kinin sensitivity in T84 cells by growth in the nude mouse, *Am. J. Physiol.*, 1991, **261**, C822–C827, DOI: 10.1152/ajpcell.1991.261.5.C822.

38 R. Alessandro, *et al.* Identification and phenotypic characterization of a subpopulation of T84 human colon cancer cells, after selection on activated endothelial cells, *J. Cell. Physiol.*, 2005, **203**, 261–272, DOI: 10.1002/jcp.20236.

39 J. I. Park, *et al.* Scaffold-Free Coculture Spheroids of Human Colonic Adenocarcinoma Cells and Normal Colonic Fibroblasts Promote Tumorigenicity in Nude Mice, *Transl. Oncol.*, 2016, **9**, 79–88, DOI: 10.1016/j.tranon.2015.12.001.

40 W. Birchmeier, J. Behrens, K. M. Weidner, J. Hulsken and C. Birchmeier, Epithelial differentiation and the control of metastasis in carcinomas, *Curr. Top. Microbiol. Immunol.*, 1996, **213**(Pt 2), 117–135, DOI: 10.1007/978-3-642-61109-4_6.

41 *Cancer Facts and Fig. 2019*, American Cancer Society, 2019.

42 E. C. Ory, *et al.* Extracting microtentacle dynamics of tumor cells in a non-adherent environment, *Oncotarget*, 2017, **8**, 111567–111580, DOI: 10.18632/oncotarget.22874.

43 E. M. Balzer, R. A. Whipple, E. H. Cho, M. A. Matrone and S. S. Martin, Antimitotic chemotherapeutics promote adhesive responses in detached and circulating tumor cells, *Breast Cancer Res. Treat.*, 2010, **121**, 65–78, DOI: 10.1007/s10549-009-0457-3.

44 G. S. Karagiannis, *et al.* Neoadjuvant chemotherapy induces breast cancer metastasis through a TMEM-mediated

mechanism, *Sci. Transl. Med.*, 2017, **9**(397), DOI: 10.1126/scitranslmed.aan0026.

45 R. A. Whipple, *et al.* Parthenolide and costunolide reduce microtentacles and tumor cell attachment by selectively targeting detyrosinated tubulin independent from NF-kappaB inhibition, *Breast Cancer Res.*, 2013, **15**, R83, DOI: 10.1186/bcr3477.

46 C. Aillaud, *et al.* Vasohibins/SVBP are tubulin carboxypeptidases (TCPs) that regulate neuron differentiation, *Science*, 2017, **358**, 1448–1453, DOI: 10.1126/science.aao4165.

47 J. Nieuwenhuis, *et al.* Vasohibins encode tubulin detyrosinating activity, *Science*, 2017, **358**, 1453–1456, DOI: 10.1126/science.aao5676.